Metallophysics and Advanced Technologies
Металофіз. новітні технол.
Metallofiz. Noveishie Tekhnol.
2026, vol. 48, No. 8, pp. 791–805
https://doi.org/10.15407/mfint.48.08.0791
Reprints available directly from the publisher

© 2026 G. V. Kurdyumov Institute for Metal Physics,
National Academy of Sciences of Ukraine
Published by license under
the G. V. Kurdyumov Institute for Metal Physics–
N.A.S. of Ukraine Publishers imprint.
Printed in Ukraine.

PACS numbers: 61.43.Dq, 61.43.Fs, 61.66.Dk, 65.60.+a, 81.05.Bx, 81.07.Bc, 81.70.Pg

Influence of Y and Al Addition on the Glass-Forming Ability of Complex Alloyed $Fe_{40–50.4}(TM, Al)_{29.1–37.5}Y_{1.8–2}(Si, C, B)_{19.7–22}$ Alloys

I. K. Yevlash, M. S. Nizameyev, I. V. Zagorulko, O. M. Semyrga, O. I. Boshko, and V. K. Nosenko

G. V. Kurdyumov Institute for Metal Physics, N.A.S. of Ukraine,
36 Academician Vernadsky Blvd.,
UA-03142 Kyiv, Ukraine

The influence of Y and Al alloying on the glass-forming ability of bulk metallic glasses of the $Fe_{40–50.4}(TM, Al)_{29.1–37.5}Y_{0–2}(Si, C, B)_{19.7–22}$ system alloys with different content of transition metals (TM) and metalloids is investigated. An extensive analysis of the amorphization tendency of the studied alloys is carried out with a comparison of the effectiveness of several criteria. In rapid-quenched bulk samples of the complex alloyed alloys studied in the article, a number of non-equilibrium structures are observed (namely, purely amorphous, amorphous–crystalline (nanocomposite) and nanocrystalline ones) that indicates a significant dependence of the structure of this group of alloys on cooling conditions. As shown, the main factor determining the amorphization tendency of Fe-based alloys is the proximity of the alloy composition to the eutectic. Alloying the alloys with yttrium and aluminium significantly increases the melt amorphization tendency.

Key words: eutectic alloys, nanocrystallization, amorphization, melt quenching, bulk metallic glasses, glass-forming ability.

Досліджено вплив леґування Y і Al на схильність до аморфізації об'ємних металевих стекол стопів системи $Fe_{40–50.4}(TM, Al)_{29.1–37.5}Y_{0–2}(Si, C, B)_{19.7–22}$ з різним вмістом перехідних металів (TM) і металоїдів. Проведено широку

Corresponding author: Igor Yevlash
E-mail: igor.yevlash@gmail.com

Citation: I. K. Yevlash, M. S. Nizameyev, O. M. Semyrga, O. I. Boshko, and V. K. Nosenko, Influence of Y and Al Addition on the Glass Forming Ability of Complex Alloyed $Fe_{40–50.4}(TM, Al)_{29.1–37.5}Y_{1.8–2}(Si, C, B)_{19.7–22}$ Alloys, *Metallofiz. Noveishie Tekhnol.*, **48**, No. 8: 791–805 (2026), DOI: 10.15407/mfint.48.08.0791

© Publisher PH 'Akademperiodyka' of the NAS of Ukraine, 2026. This is an open access article under the CC BY-ND license (https://creativecommons.org/licenses/by-nd/4.0)

аналізу схильности до аморфізації досліджуваних стопів з порівнянням ефективности кількох критеріїв. У швидкозагартованих об'ємних зразках складнолеґованих стопів, досліджених у роботі, спостерігається ряд нерівноважних структур, а саме, повністю аморфні, аморфно-кристалічні (нанокомпозитні) та нанокристалічні, що свідчить про значну залежність структури цієї групи стопів від умов охолодження. Показано, що основним чинником, що визначає схильність до аморфізації стопів на основі Fe, є близькість складу стопу до евтектики. Леґування стопів Ітрієм і Алюмінієм значно підвищує схильність до аморфізації розтопу.

Ключові слова: евтектичні стопи, нанокристалізація, аморфізація, загартування розтопів, об'ємні металеві стекла, здатність до склоутворення.

(Received 21 April, 2025; in final version, 3 March, 2026)

1. INTRODUCTION

The development and use of bulk metallic glasses (BMGs) are of significant interest to modern scientists. Currently, BMGs, which are produced by melt quenching at rates ≤ 100 K/s, have been obtained in alloys based on Zr, Pd, Mg, Ti, Ni, Fe [1, 2]; among these BMGs, iron-based alloys occupy a special place both from a commercial and technological point of view, since they have a unique combination of relatively low cost with high strength characteristics, wear resistance, corrosion resistance, magnetic and even antibacterial properties [3–5]; the competitiveness of bulk amorphous alloys (BAAs) also depends on their amorphization tendency, strength characteristics in combination with satisfactory plasticity, corrosion resistance, thermal stability of the structure, and manufacturing technological regimes, which should be as close as possible to traditional casting technologies.

For the development of BAAs, modern researchers mainly use topological criteria for the glass forming ability of metal melts [6]; one such criterion is a large ($\geq 12\%$) difference in the atomic diameters of the alloy components, number of which there must be at least three [1]; the second criterion emphasizes that the atomic sizes of the alloy components and their concentrations must correspond to certain ratios that provide the densest packing of atoms in the disordered structure [6]; according to Turnbull's thermodynamic criterion [7], the glass forming ability of the alloy increases with increasing normalized glass transition temperature $T_{rg} = T_g/T_l$, where T_g and T_l are the glass transition and liquidus temperatures, respectively; to reduce T_l of iron-based alloys, it is necessary to add metalloid alloy to them, as well as some refractory metals (Zr, Nb, Mo, *etc.*); the addition of refractory metals also contributes to an increase in the glass transition temperature due to an increase in elastic moduli [8]; according to the results of experimental studies of the influence of alloying elements on the glass form-

ing ability of iron-based alloys, it was found that small (1.5–2 at.%) additions of yttrium and other rare earth metals have the most effective effect on reducing the critical cooling rate; thus, the critical thickness of amorphous castings of $Fe_{50}Cr_{14}Mo_{14}C_{14}B_6Y_2$ and $Fe_{50}Cr_{14}Mo_{14}C_{14}B_6Dy_2$ alloys is of 4 mm [9], $Fe_{60}Cr_{10}Mo_9C_{10}B_6Er_2Ni_3$ alloy is of 8 mm [10], $(Fe_{44.3}Cr_5Co_5Mo_{12.8}Mn_{11.2}C_{15.8}B_{5.9})_{98.5}Y_{1.5}$ and $(Fe_{44.3}Cr_{10}Mo_{12.8}Mn_{11.2}C_{15.8}B_{5.9})_{98.5}Y_{1.5}$ alloys is of 12 mm [11], and $Fe_{41}Co_7Cr_{15}Mo_{14}C_{15}B_6Y_2$ alloy is of 16 mm [12]; such critical thickness values of BAAs are record-breaking at the present time; partial replacement of Fe with other transition metals has a less pronounced effect on the amorphization tendency of alloys: the critical thickness of the $Fe_{64}Mo_{14}C_{15}B_7$ alloy casting increases from 2.5 to 4 mm when alloyed with Mn, Cr, and W ($Fe_{49}Mn_{10}Mo_{14}Cr_4W_1C_{16}B_6$) [13], and a change in the Fe/Co ratio from 9:1 in the $[(Fe_{0.9}Co_{0.1})_{0.75}B_{0.2}Si_{0.05}]_{96}Nb_4$ alloy to 1:1 leads to an increase in the critical thickness of the ingots from 2 to 5 mm [14].

The strength properties of BAAs are an important criterion from the competitiveness point of view. As it known, amorphous metal alloys are characterized by a high level of hardness, strength, and wear resistance [15] due to the disordered nature of their structure, in which there are no defects in the crystal structure. Among the known amorphous metal alloys, the strongest are alloys based on the Fe–B system. Their strength limit exceeds 3500 MPa [15]. The level of mechanical properties of amorphous metal alloys largely depends on changes in their chemical composition. For example, an increase in the B content to 17.5 at.% in the $Fe_{75}Si_{10}B_{15}$ alloy instead of Fe causes an increase in the strength limit to 3900 MPa [16]. Therefore, research is focused on finding such combinations of alloying elements that would simultaneously increase the level of both strength properties and the amorphization tendency of alloys. For Fe-based alloys, the optimal alloying elements are Co and Nb, the addition of which made it possible to create a number of high-strength alloys of the $[(Fe_{1-x}Co_x)_{0.75}B_{0.2}Si_{0.5}]_{96}Nb_4$ composition with a compressive strength limit of 3900–4250 MPa, which are amorphized in the form of rods with a diameter of 2 to 5 mm [17, 18].

An additional potential for increasing the strength properties of BAAs is the formation of crystalline phases in the initial amorphous matrix [16, 19], as was observed, for example, in amorphous alloys based on Al [20]. However, currently for Fe-based alloys, this issue remains almost unexplored.

Thus, based on the analysis of literature data, it can be concluded that the problem of creating a new class of structural materials, *i.e.*, bulk amorphous alloys, is extremely relevant, but far from resolved. Further comprehensive research is needed, aimed at finding new alloy compositions with increased characteristics of glass forming ability,

thermal stability, strength, and plasticity, as well as reduced sensitivity to the purity of components and casting conditions.

Based on the above, the main idea of this study was to establish the influence of chemical composition (alloying with yttrium and aluminium) and production conditions on the amorphization and nanocrystallization tendency of complex alloyed iron-based alloys for further development of high-strength composites.

2. EXPERIMENTAL/THEORETICAL DETAILS

Research and development of methods for rapid melt quenching were carried out on alloys of the $Fe_{40-50.4}(TM, Al)_{29.1-37.5}Y_{0-2}(Si, C, B)_{19.7-22}$ system with different content of transition metals and metalloids, the chemical compositions and markings of which are given in Table 1.

The alloys were synthesized (melted) taking into account the physicochemical approach [21] to predict facilitated glass formation, which is based on the properties of the alloy components and the features of their interaction, reflected in the phase diagrams. In particular, the formation of glasses is facilitated by the presence of deep eutectics on binary (Fe–B, Fe–P) and ternary (Fe–B–Si, Fe–P–C) phase diagrams, a significant (not less than 15%) difference in the atomic diameters of the components (transition metals and metalloids), a large difference in their valence [7, 22, 23], as well as the presence in each alloy of significantly more than three components with large negative enthalpies of mixing (ΔH^{mix}). In general, variations in the composition of alloyed alloys were carried out to increase their ability to amorphized and processability during casting (quenching, including ultrafast) on air.

When obtaining bulk amorphized ingots (plates and rods) of new alloys, made by refining from the initial industrial alloys and raw materials, it was shown that the method of casting the melt under excess

TABLE 1. Marking and chemical composition of the studied alloys.

No.	Alloy mark	Chemical composition, at.%	Total metalloid content, at.%
1	HBRM-4	$Fe_{60.6}Cr_{13.8}Mn_{0.3}Mo_{1.9}Nb_2Al_{0.2}Cu_{0.5}B_{16.2}C_2Si_{2.5}$	20.7
2	HBRM-4-1	$Fe_{58.5}Cr_{14.1}Mn_{0.3}W_{1.9}Mo_3Nb_{0.9}Al_{0.1}Cu_{0.5}B_{17.1}C_2Si_{1.6}$	20.7
3	HBCY-1	$Fe_{49.7}Co_{4.5}Cr_{14.7}Mo_{9.3}B_{3.6}C_{13.5}Si_{4.6}Al_{0.1}$	21.7
4	HBCY-1-1	$Fe_{40}Co_{5.3}Cr_{16.6}W_{3.9}Mo_{10.5}Mn_{0.2}B_4C_{14.9}Si_{1.7}Al_1Y_{1.9}$	20.6
5	HBCY-2	$Fe_{50.4}Co_{4.5}Cr_{14.8}Mo_{9.3}Mn_{0.4}B_9C_9Si_{2.5}Al_{0.1}$	20.5
6	HBCY-2-1	$Fe_{43.6}Co_{5.4}Cr_{15.9}W_{3.9}Mo_{7.9}Mn_{0.6}B_{9.8}C_{9.8}Si_{0.1}Al_1Y_2$	19.7
7	HBCY-3	$Fe_{42.4}Co_{6.6}Cr_{15.6}Mo_{13.4}B_{5.8}C_{14.6}Si_{1.6}$	22
8	HBCY-3-1	$Fe_{41.6}Co_{7.1}Cr_{15.3}Mo_{12.8}B_{5.9}C_{14.8}Si_{0.6}Al_{0.1}Y_{1.8}$	21.3

TABLE 2. List of studied samples and their cooling rates calculated using empirical equations from works [26–30].

Alloy mark	Ribbon thickness, μm	Evaluated speed, K/s	Bulk samples	Evaluated speed, K/s
HBRM-4	20	5.85×10^6	Plates–3/5 mm	340/208
HBRM-4-1	19	5.92×10^6	Plates–3/5 mm	340/208
HBCY-1	28	2.06×10^6	Plates–2/5 mm	505/340
HBCY-2	25	2.93×10^6	Plates–2/5 mm	505/340
HBCY-3	28	2.06×10^6	–	–
HBCY-1-1	40	6.82×10^5	Rod–3.8 mm	414
HBCY-2-1	30	1.66×10^6	Rod–3.5 mm	448
HBCY-3-1	–	–	Plate–3.6 mm	448

pressure (higher than 0.5 atm.) into a copper mould with a thickness of 2–3 mm in a protective atmosphere of argon or helium makes it possible to obtain them almost completely in an amorphous state for rods with a diameter of 3–3.5 mm, made of complex alloyed alloys HBCY-1-1 and HBCY-2-1 containing yttrium and aluminium.

Thus, the obtained rapidly cooled samples, the list of which is given in Table 1, had the form of ribbons, plates and rods of various thicknesses.

Using the $R(D)$ dependences [24–27] for different ranges of thicknesses, as well as taking into account the difference in the cooling rate of ingots in the form of plates and rods with the same values of thickness and diameter according to the geometric parameters of all the studied strip and bulk samples studied in this work, the cooling rates were calculated, which, together with the list of samples, are given in Table 2.

3. RESULTS AND DISCUSSION

X-ray studies of rapidly cooled ribbons showed that their diffraction patterns had a form typical of amorphous metal alloys (Fig. 1).

Analysis of the angular positions of the scattering maxima, the heights of the first maximum $I(2\theta)$ and the interatomic distances r_1 showed that for the ribbons of all the studied alloys in the initial state the atomic structure is quite similar. The dimensions of the CSR(L) calculated from these data are within 1.11–1.61 nm (Table 3), which is also typical for metallic glasses. This indicates that the technological parameters of the melt-spinning method used in this work provided cooling rates sufficient to suppress completely the crystallization process in the studied melts. The obtained values of L of the initial amorphous ribbons for different groups of alloys do not correlate with the

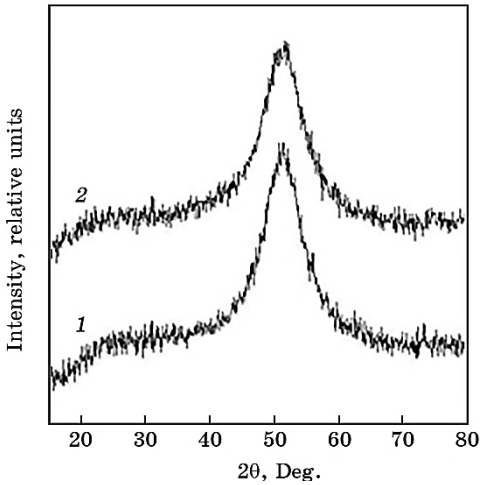


Fig. 1. Diffraction patterns of rapidly cooled ribbons of alloys: HBCY-1 (*1*) and HBCY-2 (*2*).

TABLE 3. Structure parameters of the studied alloys.

Alloy mark	Half-width of halo, deg.	$2\theta_B$, deg.	CSR dimension, L, nm (fraction, X)	Average interatomic distance, nm
HBRM-4	9.28365	52.38	1.23	0.249
HBCY-1	7.05809	51.44	1.61	0.254
HBCY-2	7.62558	51.38	1.49	0.254
HBCY-2-1	10.260	51.123	1.11	0.255

chemical composition and their tendency to amorphization. Thus, the minimum dimensions of the CSR obtained both for ribbons of the yttrium-doped alloy HBCY-2-1 (1.11 nm) with a high and for HBRM-4 (1.23 nm) with a low tendency to amorphization.

From a physical point of view, the most accurate quantitative characteristic of the melt tendency to amorphization (TA) is the minimum (critical) cooling rate, R_c, at which the experimentally detectable fraction of the crystalline phase (usually $\leq 1\%$) does not have time to form in the melt.

However, these measurements are quite complex and to date, experimentally determined R_c for bulk metal alloys (BMAs) based on Fe have been given only in a few works. The data available in the literature on the amorphization of a wide range of metal melts have allowed us to establish empirical correlations between the values of R_c and D_c and a number of thermodynamic criteria characterizing the tendency of melts to glass formation [22]. In particular, qualitative criteria for the

tendency are the relative glass-transition temperature $T_{ra} = T_a/T_l$, the temperature range of the existence of a supercooled melt $T_{ons} - T_a$, and the ratio $y_m = (2T_{ons} - T_a)/T_l$ [31].

By comparing the results of structural studies of a number of obtained alloys, it was found that the use of the γ criterion allows for a qualitative prediction of the critical thickness of ingots. However, the expansion of the range of alloys studied revealed certain discrepancies between the predictions made using this criterion, and further analysis of the TA given in the literature led to the development of a number of new thermodynamic criteria that more correctly characterize the conditions of melt amorphization. Based on this, in this work an extended analysis of the TA of the studied alloys was carried out with a comparison of the effectiveness of several criteria.

As TA criteria, in addition to the γ criterion, two more criteria, $y_m = (2T_{ons} - T_a)/T_l$ and $\omega = T_g/T_{ons} - 2T_g/(T_g + T_l)$, were selected, for which, in Ref. [33], the empirical dependences of the cooling rates [K/s] are given in the form $R_c(\gamma) = 1.333\times10^{21}\exp(-111.138\gamma)$, $R_c(\gamma_m) = 3.947\times10^{14}\exp(-43.802\gamma_m)$ and $R_c(\omega) = 1.833\times10^{-3}\exp(54.639\omega)$.

One of the most important characteristics of amorphous alloys is thermal stability (crystallization onset temperature T_{ons}), since it determines the temperature–time limits in which the physical properties inherent in the amorphous structure are preserved. In addition to the T_{ons} temperature, the value of which was estimated mainly at a heating rate of 10 K/min, the DSC thermograms shown in Fig. 2, contain indirect information regarding the structure of rapidly cooled ribbons and the nature of the transition of amorphous phases to the equilibrium crystalline state. As can be seen from the data presented, the transition of amorphous phases in the studied alloys begins at different temperatures and occurs in two (alloy HBRM-4, Fig. 2, *a*), three (alloys HBCY-1 HBCY-2, HBCY-3 Fig. 2, *b*), four (alloy HBCY-2-1, Fig. 2, *c*) and even in five stages (HBCY-1-1, Fig. 2, *d*).

A common feature of all thermograms of rapidly cooled ribbons of the studied alloys without exception and additional confirmation of the amorphous nature of their structure is the presence of a small endothermic effect immediately before the onset of crystallization, which is a sign of a glass transition, the quantitative characteristic of which is the glass transition temperature, T_g (temperature of the inflection point of the thermogram).

In addition to the temperatures T_g and T_{ons}, the parameter γ also includes T_l, which is an important technological characteristic of the casting process, since it significantly determines the viscosity of the melt.

A common feature of the thermograms of the studied alloys (Fig. 3) is a large endothermic effect, from which melting begins and which, with increasing temperature, is accompanied (except for alloy HBCY-2-1, Fig. 3, *b*) by a number of weaker endothermic reactions.

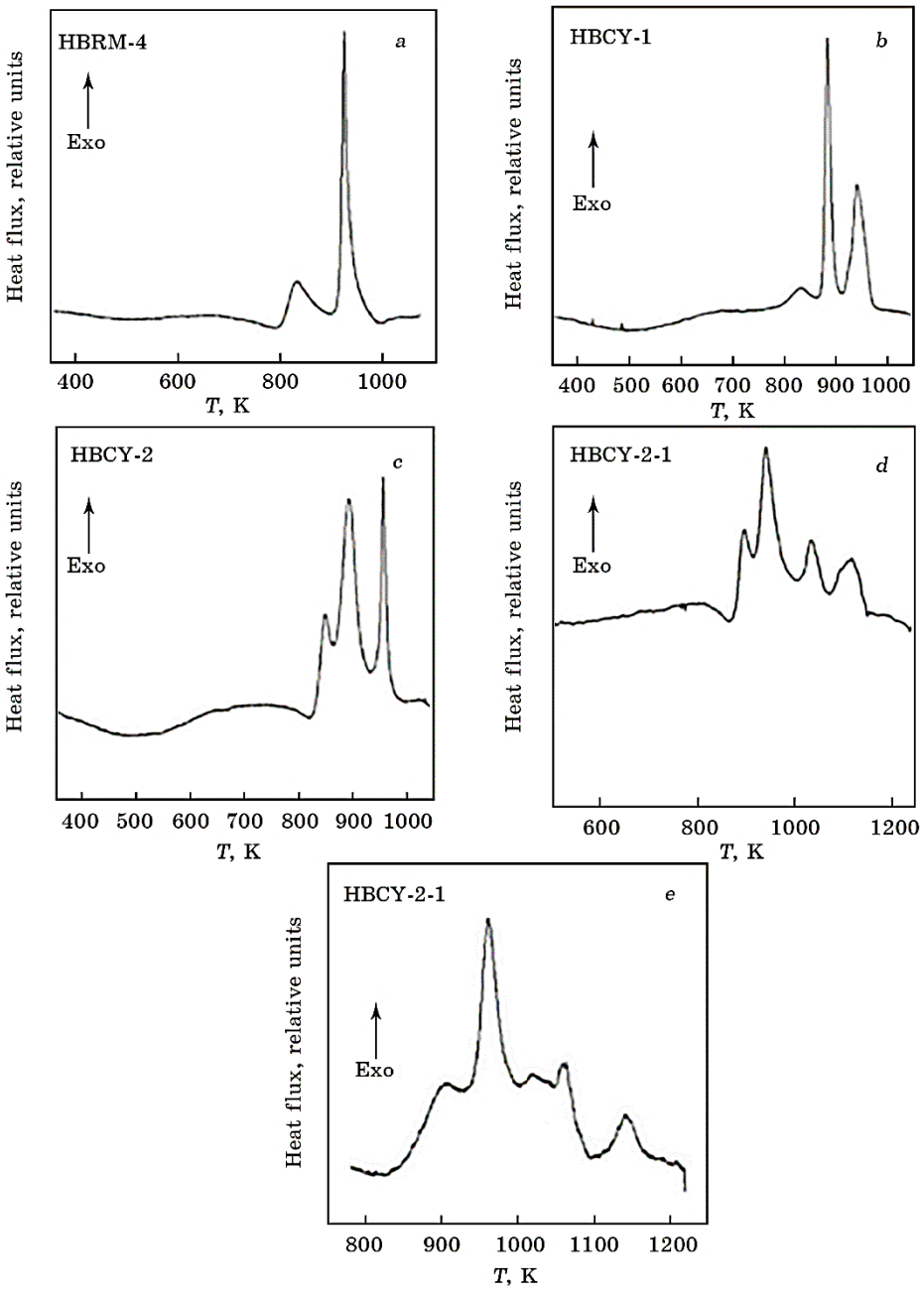


Fig. 2. DSC thermograms of amorphous ribbons of alloys of grades: crystallization in two (alloy HBRM-4) (*a*); three (alloys HBCY-1 (*b*) HBCY-2 (*c*), four (alloy HBCY-2-1) (*d*) and even in five stages (HBCY-1-1) (*e*).

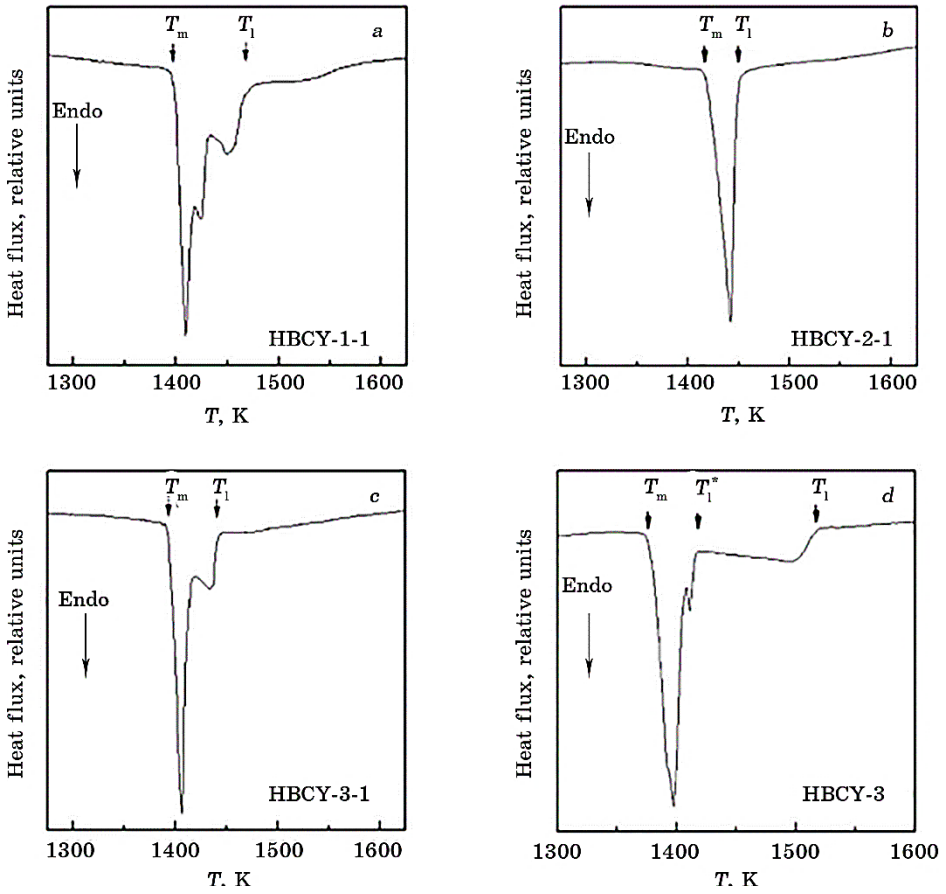


Fig. 3. Melting thermograms measured at a heating rate of 10 K/min., of the initial ingots of the studied alloys: HBCY-1-1 (*a*); HBCY-2-1 (*b*); HBCY-3-1 (c); HBCY-3 (*d*).

Thermal reactions that occur at higher temperatures correspond to the melting of carbide and boride phases, which ends at the liquidus temperature.

The T_L values estimated from these data are given in Table 4 and marked with asterisks, in contrast to the T_L measured using optical pyrometry.

From the above relationships and the data in Table 4, it follows that the differences in the values of the γ and γ_m criteria, which reflect the relative TA of the studied alloys, are due, first of all, to the differences in the liquidus temperatures (Fig. 3), the higher values of which indicate a significant deviation of the alloy composition from the eutectic.

The obtained R_c values for the HBCY-1-1, HBCY-2-1 and HBCY-3-1

TABLE 4. Thermal stability parameters of amorphous phases during continuous heating at a rate of 10 K/min; thermodynamic criteria characterizing the TA of the studied alloys; critical cooling rates and critical thicknesses.

Alloy mark	T_L, K	T_g, K	T_{ons}, K	T_g/T_L	γ	$R_c(\gamma)$, K/s	$D_c(\gamma)$, mm	γ_m	$R_c(\gamma_m)$, K/s	$D_c(\gamma_m)$,mm
HBRM-4	1320	767	798	0.58	0.382	176	2.36	0.637	300	3.417
HBCY-1	1388	762	794	0.549	0.369	813	1.37	0.595	1.89×10^3	0.267
HBCY-2	1438	807	827	0.56	0.368	825	1.34	0.589	2.47×10^3	0.245
HBCY-3	1517	849	875	0.56	0.370	765	1.4	0.594	1.98×10^3	0.263
HBCY-1-1	1467*	866	896	0.59	0.384	150	2.5	0.588	2.62×10^3	0.379
HBCY-2-1	1437*	840	874	0.585	0.384	153	2.5	0.621	614	1.639
HBCY-3-1	1429*	857	879	0.60	0.385	142	2.6	0.631	391.5	1.718

* T_l values measured from DSC thermograms

alloys doped with yttrium and aluminium are noticeably (more than 5 times) higher than for the HBCY-1, HBCY-2 and HBCY-3 alloys.

The estimates of the cooling rates of a 3.5 mm thick bar and a 3.6 mm thick plate, made using the dependence $\lg R = 8.06 - 1.69 \lg D$ [28], give values of 140 and 137 K/s, respectively, which are close to the critical cooling rates R_c for the HBCY-2-1 and HBCY-3-1 alloys (153 and 142 K/s, respectively), calculated using the thermodynamic criterion γ (Table 4). The analysis shows that the thermodynamic criterion γ can be useful for a preliminary assessment of the tendency of alloys to amorphization.

Among the alloys studied that did not contain yttrium and aluminium, both HBCY-1 and HBCY-2 are characterized by a high ability to amorphized and thermal stability of the amorphous state. For a more detailed study of the tendency of these alloys to amorphization, ingots of alloys HBCY-1 and HBCY-2 with a thickness of 2 mm were produced, but their phase compositions were practically identical to those of ingots with a thickness of 5 mm. Figure 4 shows the diffraction patterns obtained from samples cut from the lower parts of ingots with a thickness of 2 mm of alloys HBCY-1 and HBCY-2.

As can be seen from the above data, both samples have a crystal structure consisting of solid solution crystals based on α-Fe, tetragonal phase of the Fe_3B type, $Cr_{23}C_6$ type phase with a complex cubic lattice and Fe_7C_3 phase, the lattice of which belongs to the rhombic system. From the data in Fig. 4, it follows that the redistribution of amorphized elements (increasing the B concentration in the HBCY-2 alloy by 6 at.% due to 5 at.% C and 1 at. % Si) did not lead to significant changes in the phase composition of the ingots, except for a noticeable decrease in the content of Fe_7C_3 carbide.

In addition, a comparison of the diffractograms shown in Fig. 4 shows that the interference lines of α-Fe and carbides and borides

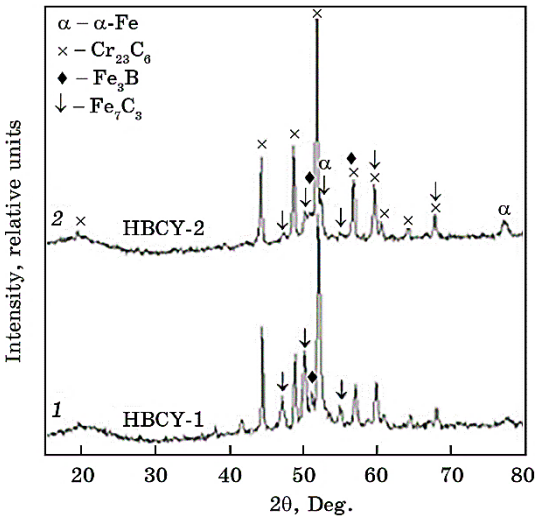


Fig. 4. Diffraction patterns of ingots (bottom) 2 mm thick of alloys HBCY-1 (B-376) (*1*) and HBCY-2 (B-379) (*2*) in the initial state (symbol ♦—lines of the tetragonal phase Fe_3B, α—α-Fe, ×—$Cr_{23}C_6$ phase, ↓—Fe_7C_3-type phase).

formed in the HBCY-1 alloy ingot are noticeably wider than in the HBCY-2 alloy ingot, which indicates a smaller size of nanocrystals in the first of these alloy.

It follows from the diffraction patterns of bulk samples of the HBCY-2-1, HBCY-3-1 and HBRM-4-1 alloy ingots shown in Fig. 5 that, despite the relatively close cooling rates, their structure is noticeably different. If the diffractogram of the HBCY-2-1 alloy ingot (Fig. 5, *a*) contains only a diffuse maximum, which is typical for bulk metallic glasses, then in the diffraction patterns of the remaining samples, reflections from crystalline phases are observed: in the HBCY-3-1 alloy against the background of the maximum from the amorphous phase (Fig. 5, *b*), while in the patterns of the HBRM-4-1 alloy (Fig. 5, *c*) no signs of amorphousness are observed.

Calculations of the relative fraction of the crystalline phase, X, and estimation of the crystal size showed that the structure of the HBCY-3-1 alloy plate contains approximately 10% α-Fe crystals, the average size of which is 12.4 nm, and the bulk density is 10^{23} m^{-3}. Such parameters are typical for the so-called nanocomposite structures that are formed during partial crystallization of amorphous phases upon heating, which was observed, in particular, in amorphous ribbons of the HBRM-4 alloy [33]. The surface layers of the HBCY-3-1 plate contained a small amount of ultrafine (nanosize) carbides and borides identified (marked) on the diffractogram. By gradually grinding the HBCY-3-1 plate, it was possible to establish that all the detected nano-

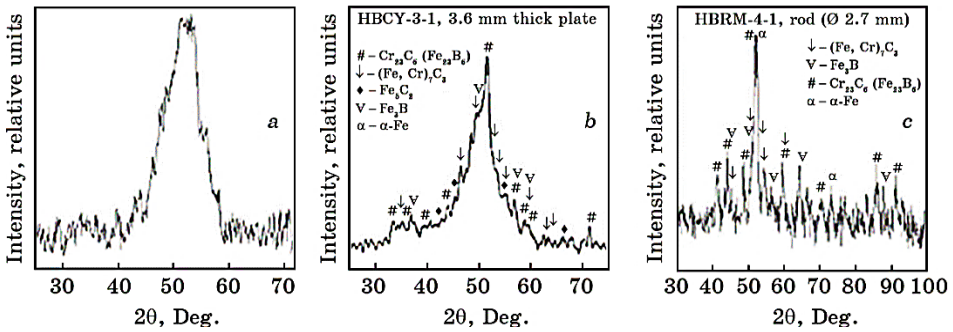


Fig. 5. Diffractograms (CoK_α radiation) of rapidly-cooled bulk alloy samples: *a*—HBCY-2-1 (rod with a diameter of 3.5 mm); *b*—HBCY-3-1 (plate with a thickness of 3.6 mm); *c*—HBRM-4-1 (rod with a diameter of 2.7 mm).

crystals were formed in its surface layer. The presence of an amorphous phase in the inner layers of the ingots and its smaller amount on the surface is at first glance somewhat unexpected, since the surface layers are cooled in direct contact with the walls of the copper casting mould at a higher rate. Nevertheless, a similar effect (formation of crystalline layers on the surface of the castings) was observed in a number of works when obtaining ingots from bulk amorphized alloys based on Fe [34] and Zr [35].

The structure of the HBRM-4-1 alloy ingot consists of α-Fe crystals and phases isomorphic to the borides $Cr_{23}C_6$ ($Fe_{23}B_6$), Fe_3B and $(Fe, Cr)_7C_3$. The estimates showed that the average size of α-Fe crystals and $Fe_{23}B_6$ boride in the structure of the HBRM-4-1 alloy rod is 19.0 and 32.0 nm, respectively.

As a generalization of the results of the structural analysis, we note that in the bulk rapidly cooled samples of complex alloyed alloys of the studied system (Fe, Co)–(Cr, Mo, W, Nb)–Y–(C, B, Si, Al), a number of non-equilibrium structures are observed: purely amorphous (HBCY-2-1), amorphous–crystalline (nanocomposite) (HBCY-1, HBCY-2, HBCY-3-1) and nanocrystalline (HBRM-4, HBRM-4-1), which indicates a significant dependence of the structure of this group of alloys on the cooling conditions. Doping of alloys with Y and Al noticeably increases the tendency of melts to amorphization, which is probably associated both with the optimization of the atomic packing density in the melt due to the addition of large atoms, and with the formation of an oxide protective film on the surface of the solidifying melt.

It is expected that active development of technological processes for casting amorphous Fe-based alloys, close to industrial ones, as well as the use of technical purity components and alloys as starting materials, will reduce the cost of a new class of materials with unique sets of properties to the level of existing tool steels. Further developments in

this direction should be aimed at creating and developing a high-performance technology for the industrial production of highly-alloyed volume-strengthened structural nanostructured materials by controlled crystallization of melts, amorphous ribbons and bulk ingots of developed iron-based alloys; development of a technology for manufacturing electrodes from nanophase powder for applying wear-resistant coatings using existing technologies.

4. CONCLUSIONS

1. The main factor determining the TA of Fe-based alloys is the proximity of the alloy composition to the eutectic one. According to the results of the evaluations, the alloys doped with yttrium and aluminium HBCY-1-1 ($Fe_{40}Co_{5.3}Mn_{0.2}Cr_{16.6}W_{3.9}Mo_{10.5}B_4C_{14.9}Si_{1.7}Al_1Y_{1.9}$), HBCY-2-1 ($Fe_{43.6}Co_{5.4}Mn_{0.6}Cr_{15.9}W_{3.9}Mo_{7.9}B_{9.8}C_{9.8}Si_{0.1}Al_1Y_2$) and HBCY-3-1 ($Fe_{44.85}Co_{7.1}Mn_{0.05}Cr_{15.3}W_{0.01}Mo_{12.8}B_{5.9}C_{14.8}Si_{0.6}Al_{0.1}Y_{1.8}$) have the highest tendency to glass formation, with critical ingot thicknesses of 2.5, 2.5 and 2.6 mm, respectively.
2. The main reason for the presence of nanocrystalline phases in the surface layers of the HBCY-3-1 thin plate and their absence in the inner layers is the intensive heterogeneous nucleation of crystals in the surface layers, caused by their interaction mainly with oxygen residues in the casting atmosphere during a relatively long cooling time. Reducing the influence of heterogeneous nucleation can be achieved by improving the casting conditions (in particular, by choosing the atmosphere), as well as by selecting alloying impurities that reduce the nucleation rate.
3. In the bulk rapidly cooled samples of complex alloyed alloys of the studied system (Fe, Co)–(Cr, Mo, W, Nb)–Y–(C, B, Si, Al), a number of non-equilibrium structures are observed: purely amorphous (HBCY-2-1), amorphous–crystalline (nanocomposite) (HBCY-1, HBCY-2, HBCY-3-1) and nanocrystalline (HBRM-4, HBRM-4-1), which indicates a significant dependence of the structure of this group of alloys on the cooling conditions.

AUTHORS' CONTRIBUTIONS

Y.I.K. wrote the manuscript with input from all authors, performed numerical calculations of x-ray diffractograms. N.M.S. synthesized (melted) initial alloys, carried out rapid quenching of ribbons and bulk samples, reviewed the literature and collected data. Z.I.V. conducted DSC studies of rapidly quenched samples. B.O.I measured the mechanical properties, provided heat treatments. S.O.M. supervised the findings of this work. N.V.K. supervised the project, devised the main con-

ceptual ideas, verified analytical approaches, and provided critical feedback. All authors approved the final version of the manuscript.

REFERENCES

1. J. P. Chu, J. E. Greene, J. S. C. Jang, J. C. Huang, Y.-L. Shen, P. K. Liaw, Y. Yokoyama, A. Inoue, and T.G. Nieh, *Acta Mater.*, **60**, Nos. 6–7: 3226 (2012).
2. M. Chen, L. Zhu, Y. Chen, S. Dai, Q. Liu, N. Xue, W. Li, J. Wang, Y. Huang, K. Yang, and L. Shao, *Materials*, **17**: 1699 (2024).
3. A. Inoue, B. L. Shen, H. Koshiba, H. Kato, and A. R. Yavari, *Acta Mater.*, **52**, No. 6: 1631 (2004).
4. J. Lu, Y. Li, S. Ma, W. Li, F. Bao, Z. Zhu, Q. Zeng, H. Zhang, M. Yao, and W. Zhang, *Acta Metall. Sin. (Engl. Lett.)*, **37**, No. 9: 1 (2024).
5. L. Jiang, X. Fan, Q. Li, X. Li, T. Jiang, and Q. Wei, *Inorganics*, **13**, No. 4: 105 (2025).
6. O. N. Senkov and D. B. Miracle, *Mater. Res. Bull.*, **36**: 2183 (2001).
7. M. Marcus and D. Turnbull, *Mater. Sci. Eng.*, **23**: 211 (1976).
8. T. Egami, *Mater. Sci. Eng. A*, **226–228**: 261 (1997).
9. M. Iqbal, J. I. Akhtar, H. F. Zhang, and Z. Q. Hu, *J. Non-Cryst. Sol.*, **354**: 3284 (2008).
10. Y. H. Zhao, C. Y. Luo, X. K. Xi, D. Q. Zhao, M. X. Pan, and W. H. Wang, *Intermetallics*, **14**: 1107 (2006).
11. Z. Zhang, P. Sharma, and A. Makino, *J. Appl. Phys.*, **112**: 103902 (2012).
12. J. Shen, Q. Chen, J. Sun, H. Fan, and G. Wang, *Appl. Phys. Lett.*, **86**: 151907 (2005).
13. A. Makino, *IEEE Trans. Magn.*, **48**, No. 4: 1331 (2012).
14. A. Makino, T. Kubota, K. Yubuta, and A. Inoue, *J. Appl. Phys.*, **109**: 07A302 (2011).
15. I. V. Zolotukhin, *Fizicheskie Svoistva Amorfnykh Metallicheskikh Materialov* [Physical Properties of Amorphous Metallic Materials] (Moskva: Metallurgiya: 1986) (in Russian).
16. J. Fornell, S. González, E. Rossinyol, S. Suricach, M. D. Bary, D. V. Louzguine-Luzgin, J. H. Perepezko, J. Sort, and A. Inoue, *Acta Mater.*, **58**: 6256 (2010).
17. B. Shen, A. Inoue, and C. Chang, *Appl. Phys. Lett.*, **85**, No. 21: 4911 (2004).
18. A. Inoue, B. L. Shen, and C. T. Chang, *Acta Mater.*, **52**: 4093 (2004).
19. A. V. Sergueeva, N. A. Mara, D. J. Branagan, and A. K. Mukherjee, *Mater. Lett.*, **61**: 1465 (2007).
20. A. Inoue, *Progr. Mater. Sci.*, **43**: 365 (1998).
21. Yu. K. Kovneristy, E. K. Osipov, and E. A. Trofimova, *Fiziko-Khimicheskie Osnovy Sozdaniya Amorfnykh Metallicheskikh Splavov* [Physicochemical Principles of Creating Amorphous Metal Alloys] (Moskva: Nauka: 1983) (in Russian).
22. A. Inoue, *Acta Mater.*, **48**: 279 (2000).
23. S. C. Glade, R. Busch, D. S. Lee, W.L. Johnson, R. K. Wunderlich, and H. J. Fecht, *J. Appl. Phys.*, **87**: 7242 (2000).
24. J. H. Perepezko and K. Hildal, *Phil. Mag.*, **86**, No. 24: 3681 (2006).
25. K. Hildal, N. Sekido, and J. H. Perepezko, *Intermetallics*, **14**: 898 (2006).

26. Zh. Long, H. Wei, Y. Ding, X. Liu, and Z. Liu, *J. Alloys Comp.*, **475**: 207 (2009).
27. A. Inoue and A. Takeuchi, *Mater. Trans.*, **43**, No. 8: 1892 (2002).
28. A. B. Lysenko, G. V. Borisova, and O. L. Kravets, *Fiz. Tekh. Vys. Davl.*, **14**, No. 1: 44 (2007).
29. V. K. Nosenko, A. Yu. Rudenko, T. N. Moiseeva, M. S. Nizameev, A. I. Limanovskii, O. M. Semyrga, and V. I. Tkach, *Metallofiz. Noveishie Tekhnol.*, **37**, No. 12: 1681 (2015).
30. V. I. Tkatch, A. L. Limanovskii, S. N. Denisenko, and S. G. Rassolov, *Mater. Sci. Eng. A*, **323**: 91 (2002).
31. Z. P. Lu and C. T. Liu, *Acta Mater.*, **50**: 3501 (2002).
32. Zh. Long, H. Wei, Y. Ding, X. Liu, and Z. Liu, *J. Alloys Comp.*, **475**: 207 (2009).
33. A. Yu. Rudenko, V. K. Nosenko, V. I. Tkach, and M. S. Nizameev, *Metallofiz. Noveishie Tekhnol.*, **34**, No. 6: 771 (2012).
34. C. Y. Luo, Y. H. Zhao, X. K. Xi, G. Wang, D. Q. Zhao, M. X. Pan, W. H. Wang, and S. Z. Kou, *J. Non-Cryst. Sol.*, **352**: 185 (2006).
35. G. E. Abrosimova, A. S. Aronin, Yu. V. Kir'yanov, D. V. Matveev, V. V. Molokanov, and I. I. Zver'kova, *J. Non-Cryst. Sol.*, **288**: 121 (2001).